Work function and affinity changes associated with the structure of hydrogen-terminated diamond (100) surfaces

G. R. Brandes*
Advanced Technology Materials, Inc., Danbury, Connecticut 06810

A. P. Mills, Jr.
Bell Laboratories, Lucent Technologies, Murray Hill, New Jersey 07974
(Received 12 February 1998; revised manuscript received 13 May 1998)

The positron and electron work functions and affinities of diamond (100) surfaces were measured using positron reemission and Kelvin probe techniques to reveal changes in the chemical potential, surface dipole, and band bending. The positron affinity χ_+ is negative; at temperatures between 20 and 100 °C we find $\chi_+ = -4.20 \pm 0.04$ eV for the (2×1) reconstructed, hydrogen-free surface, -3.76 ± 0.04 eV for the monohydride surface, and -3.03 ± 0.04 eV for a fully hydrogenated surface. Similar magnitude, but opposite sign changes are observed for the electron work function φ_-. The increases in the room-temperature values of χ_+ and the decreases in φ_- as hydrogen is added are in agreement with theoretical results. The positron affinity of the (2×1) surface is nearly temperature independent, indicative of a surface that is nearly hydrogen-free and consisting of π-bonded dimers. As the temperature is raised, the positron affinity of the monohydride surface decreases to a minimum of -4.08 eV at (575 ± 50) °C and returns to the room-temperature value by 800 °C. We speculate that the complex temperature dependence is caused by fluctuations or phase transitions of the two-dimensional array of hydrogen atoms. Contrary to assumptions that band bending is the major contribution to changes in the contact potential of diamond, little band bending is evident at room temperature for variously prepared undoped diamond surfaces. Nevertheless, substantial changes in the positron yield at elevated temperatures are consistent with the formation of a positive electric field due to 3×10^{10} cm^{-2} surface electrons occupying states associated with absorbed oxygen or structural defects. [S0163-1829(98)02832-X]

I. INTRODUCTION

The dipole potential $\Delta\phi$ associated with various surfaces is sensitive to subtle structure and chemical changes. Comparisons of measurements of $\Delta\phi$ with theoretical predictions of $\Delta\phi$ can be one of several indicators of the quality of a surface model. Diamond[1] being the simplest elemental semiconductor and the paradigm for silicon and other industrially important materials, is in principle ideal for studies of the surface dipole. To understand the low-pressure growth of diamond by chemical vapor deposition (CVD) it is essential to understand the diamond surface structure and composition. Furthermore, diamond shows promise as a cathode material for display, spectrometer, and accelerator applications.[2]

Any measurements attempting to extract the surface dipole must carefully take into account effects due to band bending and chemical potential shifts. In the present paper, we combine a set of positron and electron measurements that enables us to distinguish all three components and arrive at unambiguous values for the surface dipole potential differences of various diamond (100) surfaces.

The C(100) surface has two dangling bonds per surface carbon atom. Because the surface is generally prepared in a hydrogen-rich environment, some fraction of the dangling bonds is likely to be hydrogen terminated. Possible surface structures (Fig. 1) include the dihydride C(100) (1×1):2H, the monohydride C(100) (2×1):2H, and the hydrogen-free, π-bonded C(100) (2×1); coverage intermediate between the monohydride and dihydride has also been hypothesized.[3]

A (2×1) low-energy electron diffraction (LEED) pattern is observed for a surface prepared by plasma-assisted diamond growth[4] or by heating the sample to 800 °C and exposing the surface to hydrogen plasma for several hours.[5] A (1×1) LEED pattern[6] is visible for a surface prepared by *ex situ* polishing, hot acid cleaning, or by some CVD diamond growth techniques.[7] Regardless of the initial structure, a (2×1) LEED pattern is obtained after heating the diamond to greater than 1000 °C, although acid-etched samples occasionally do not reconstruct or reconstruct incompletely.

The diamond surface prepared by heating to greater than 1000 °C is free of hydrogen and consists of π-bonded dimers.[8–10] Surfaces prepared *ex situ* by microwave assisted CVD (Ref. 4) or hydrogen plasma exposure[5,7,11] and subsequently annealed *in situ* at temperatures up to 450 °C were found to be (2×1) monohydride terminated. Although surfaces prepared by polishing, acid cleaning, and hot filament assisted CVD diamond growth generally show a (1×1) LEED pattern, these surfaces also contain regions of monohydride-terminated dimer pairs.[7] The long-range order of the dimer pairs is limited, however, and the (1×1) LEED pattern is thought to arise from the underlying lattice.

Dosing the hydrogen-free (2×1) surface with atomic hydrogen created by a hot filament creates a surface that gives a (1×1) LEED pattern with increased surface roughness compared to a surface prepared by exposure to hydrogen plasma.[11,12] Because hydrogen is relatively inefficient at breaking the dimer bond, exposing the surface to small doses of hydrogen does not always create enough disorder to produce a (1×1) LEED pattern.[8,9,13]

Whether a C(100) surface may contain more than one hydrogen per surface carbon atom is a subject of continuing

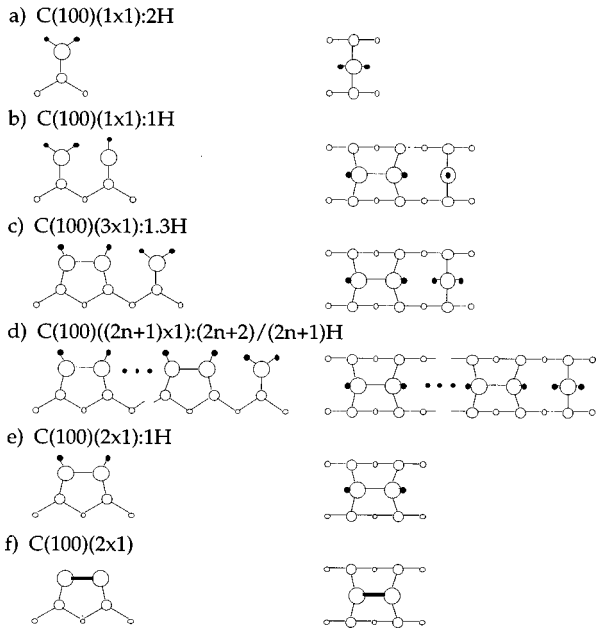

FIG. 1. Models of the surface structure of hydrogen-terminated diamond (100): (a) dihydride terminated, (b) alternating dihydride terminated and monohydride terminated atoms, (c) alternating monohydride terminated dimer and dihydride terminated atoms, (d) (2n) monohydride dimers and a dihydride terminated atom, (e) monohydride terminated dimers, (f) π-bonded dimers. The closed circles represent hydrogen atoms; the open circles with different diameters represent successive layers of carbon atoms.

discussion. Hamza *et al.* have argued, based on electron stimulated desorption measurements and temperature programmed desorption measurements, that the two dangling bonds per surface carbon atom are hydrogen terminated.[14] The results of theoretical studies[3,15,16] have indicated that the formation of the C(100)(1×1):2H is inhibited by steric crowding of H atoms on adjacent carbon atoms. The steric hindrance can be reduced by having alternating monohydride dimer and dihydride units, producing a (3×1) surface structure but without long-range order.[3] Extending this result, a whole family of $[(2n+1)\times1]$ structures separated by a dihydride unit should be possible, but the likely surface disorder would inhibit observing the corresponding $[(2n+1)\times1]$ LEED pattern. Verwoerd's calculations showed that the dihydride will not be present at high temperatures, although it may be metastable at low temperatures.[17]

An understanding of the surface structure and chemical composition is key to understanding the emission of electrons into vacuum states. The observation of a peak at the conduction-band minimum in the photoemission spectrum of the (2×1):1H diamond (100) surface indicated that this surface had a negative electron affinity[18] (NEA); theoretical studies indicated that the hydrogen-terminated surface will have a negative affinity while a hydrogen-free surface will have a positive affinity. Ultraviolet photoemission spectroscopy (UPS) studies showed the NEA disappeared after heating to >1100 °C [(2×1) surface], but reappeared upon exposure to hydrogen plasma;[10,13] a 2 eV or greater shift in the electron affinity was observed. Mearini, Krainsky, and Dayton showed that the high secondary electron yield, expected from the NEA diamond surface, dropped after the surface was dehydrogenated.[19]

We are also interested in exploring the C(100) surface to better understand the higher than expected electrical conductivity of polycrystalline diamond.[20–22] The effect is a consequence of the surface because oxidizing the diamond reduces the electrical conductivity. Shirafuji and Sugino have speculated that the surface bands have bent substantially and the surface is in accumulation, producing a conducting channel.[23]

In the present paper, we examined the positron and electron work functions and affinities of the diamond (100) surfaces using positron reemission and Kelvin probe techniques. We found the (100) surfaces of diamond have a negative affinity for positrons. Positrons implanted into the diamond are reemitted with a narrow energy spread that makes it possible to measure the positron affinity χ_+ and consequently, study changes in diamond's dipole potential. We observe a reversible temperature effect on the work function of the monohydride diamond that might be associated with fluctuations or changes in the two-dimensional surface structure. We also observe that the positron affinity is small and the electron affinity is large for as-prepared surfaces that have been heated to low temperature (<250 °C), results consistent with a surface that contains substantially more hydrogen than the monohydride surface. Kelvin probe measurements of the electron work function of a boron-doped diamond, and hence the surface dipole, agree with the positron data where a comparison is possible. The reemitted positron yield increases substantially with increasing temperature, consistent with the formation of a large surface electric field associated with the filling of surface states having their origin in oxygen or structural defects.

Before discussing in detail our experiments and experimental results, it is useful to review electron and positron work function and affinity terms and contributions.[24] Figure 2 shows the surface band diagrams for a semiconductor crystal. The electron work function is defined as the minimum energy needed to remove an electron from the Fermi level (ε_F) deep within the bulk region of a crystal to the vacuum. The distance from the crystal must be large compared to the range of the image forces but small compared to the size of the crystal facets. In order to separate surface and bulk contributions, the work function $\varphi_- = E_{\rm vac} - \varepsilon_F$ is usually written as $\varphi_- = \Delta\phi - \mu_-$, where $\Delta\phi$ is the surface dipole potential and μ_- is the bulk chemical potential. The surface dipole is only a function of the surface structure and surface chemistry. Similarly, the positron work function $\varphi_+ = -\Delta\phi - \mu_+$, where μ_+ is the positron chemical potential, is the minimum energy required to remove a positron from the bulk into the vacuum. Note that the positron chemical potential is defined relative to a crystal reference level ϕ_c so that the surface dipole contribution is equal and opposite to the electron surface dipole contribution. In any case, the sum of the electron and positron work functions is a constant, independent of surface conditions for a given bulk material. The electron affinity χ_- is the separation between the conduction-band minimum at the surface and the vacuum level; similarly, the positron affinity χ_+ is a separation from the lowest-energy positron state near the surface and the vacuum level. In both cases, true surface states are excluded from the definition.

Figure 2(a) shows the energy levels for the case where

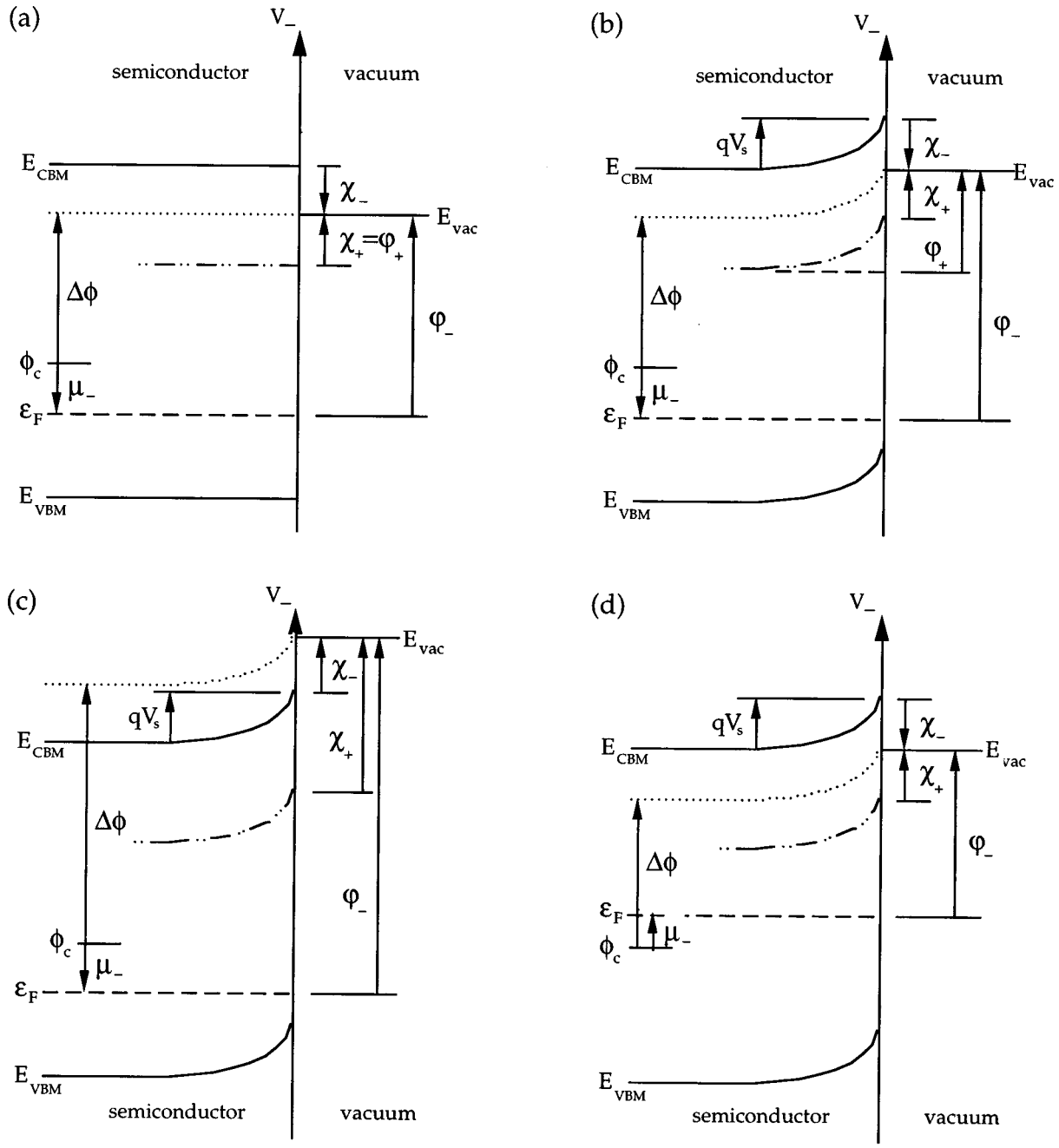

FIG. 2. Electron and positron energy levels at the semiconductor-vacuum interface: (a) flat band, (b) upwards band bending, (c) surface dipole change, and (d) chemical potential change. In the diagrams up is the direction of increasing electron energy or decreasing positron energy.

there is no band bending at the crystal surface. However, bands typically bend at semiconductor surfaces due to the presence of charges in surface states causing a near surface electric field, as shown in Fig. 2(b). The change in potential V_s that characterizes the band bending also modifies the electron work function; the electron work function is $\varphi_- = \Delta\phi - \mu_- + qV_s$.[25] Note that the electron affinity, which is defined in terms of the conduction-band minimum in the surface region, does not change when bands bend. Similarly, the positron affinity is the energy gained by moving a positron from the vacuum to the lowest bulk energy level near the surface. In metals, where there is no band bending, $\varphi_+ = \chi_+$. The positron work function is defined in terms of removing a positron from the bulk and the work function should be modified to reflect the surface band bending, that is $\varphi_+ = -\Delta\phi - \mu_+ - qV_s = \chi_+ - qV_s$. However, because our measurements are done on negative affinity surfaces by measuring the reemitted positron energy, we are observing positrons from within a few energy loss mean free paths of the surface and hence are really measuring the positron affinity. The electron and positron affinities are invariant to the presence of modest band bending.

Finally, in order to facilitate the subsequent discussion of the results, it is useful to consider how these parameters change if the surface dipole changes [Fig. 2(c)] or if the electron chemical potential changes [Fig. 2(d)]. Because the

dipole term fixes the vacuum level relative to the crystal states at the surface, changes in the dipole will produce changes in the electron and positron work functions and affinities. Alternatively, when the electron chemical potential is changed, the electron work function changes but the electron and positron affinities and the positron work function do not.

II. EXPERIMENTAL PROCEDURES

Positron reemission studies (energy and yield) and Kelvin probe studies were conducted on the C(100) surface using different experimental systems and diamonds prepared with different techniques.

Positron reemission measurement system

Positrons for the positron reemission investigations were obtained from our magnetically guided, variable energy (0.1–10 keV), ultrahigh vacuum positron beam.[26] The system base pressure was 5×10^{-11} Torr and most of the data were taken with pressures below 1×10^{-10} Torr. When heating the sample to 1025 °C the pressure rose as high as 1×10^{-9} Torr, the principal vacuum contaminant being H_2. Reemitted positrons passed through a computer-controlled electrostatic retarding field analyzer and the transmitted positrons were deflected with $E\times B$ plates into a channeltron detector. Calculations of typical charged particle trajectories through the large diameter, long drift region retarding field analyzer showed an energy resolution of better than 0.01 eV was feasible;[27] measurements indicate an energy resolution of 0.04 eV. With this configuration only the component of energy along the analyzer axis is measured. To obtain the total energy distribution of the reemitted positrons the magnetic field at the sample was increased by a factor of 5 relative to the field at the analyzer by placing a $SmCo_5$ magnet behind the sample.[28]

The sample was clamped by means of tabs to a Ta heater sheet and a thermocouple was spot welded to one of the tabs. The Ta heater sheet enabled sample heating to 1125 °C. A second thermocouple was attached to the diamond face with silver epoxy after the investigations were complete in order to determine the temperature difference between the diamond and the temperature measured at the tab.

Kelvin probe measurement system

The Kelvin probe studies were conducted in an ultrahigh vacuum surface analysis system (10^{-10} Torr) equipped with a low-energy electron diffractometer, an Auger electron spectrometer, and Kelvin probe. The sample was heated by electron beam bombardment from behind the sample holder. The Kelvin probe consists of a reference electrode that is made to vibrate in close proximity ($\sim$1 mm) to the test sample. If there is a contact potential difference between the electrode and the sample a small alternating current at the reference electrode can be detected when the electrode vibrates. The reference electrode potential is adjusted until no current is detected (the contact potential difference is zero).

The Kelvin probe electrode was a 3-mm-diameter gold grid that was made to oscillate with a piezoelectric transducer. To protect the piezoelectric transducer from damage while heating the sample, the grid arm and transducer were encased in a copper shield that was attached to a liquid-nitrogen cold finger via a copper braid. A measurement of the contact potential difference involved heating the sample to temperature then measuring the change in contact potential difference as the sample cooled (heater off). The contact potential difference could not be measured while heating because energetic electrons from the heater filament, collected by the Kelvin probe, produced an erroneous current reading.

If the reference electrode position and the work function of the reference electrode are stable, the Kelvin probe can detect changes in the contact potential difference to better than 0.01 eV. Although we were primarily interested in measuring changes in the electron work function as a function of temperature, we can determine the absolute diamond work function, although the precision of depends upon the precision with which the reference electrode is known. Saville *et al.* found the work function of polycrystalline gold that had not been cleaned was 4.2 eV,[29] as opposed to clean gold where $\varphi_- = 5.1$ eV.[30] The Au grid reference electrode was not intentionally cleaned during our measurements and consequently we assume $\varphi_-^{re} = 4.2 \pm 0.2$ eV.

Diamond surface preparation

The first diamond sample ($D1$), used in the positron reemission studies, was a synthetic, 99.9% isotopically pure ^{12}C, $6\times6\times0.5$ mm^3, (100) orientation, type IIa diamond manufactured by General Electric Superabrasives. The principal impurity in our sample was nitrogen ($<$10 ppm). The diamond sample was prepared by either of two techniques that yielded indistinguishable results for the positron affinity measurements. The first method was to immerse the diamond for 2 min in a 155 °C saturated solution of CrO_3 and H_2SO_4 followed by a rinse in an ebulliant solution containing equal parts of H_2O_2 (30%) and NH_4OH (30%).[22] The second method was to polish the diamond with a suspension of diamond grit and olive oil. Careful polishing with fine grit (0.1 μm) must be performed or positrons will be reemitted from the resulting rough surface with large transverse energies. After each preparation, the diamond was rinsed in ethyl alcohol before insertion into the vacuum system. Following an *in situ* flash to 250 °C surfaces prepared by each technique showed sharp (1×1) LEED spots. The only contaminant visible by Auger electron spectroscopy was oxygen, and an atomic concentration of no more than 4% of three monolayers was observed. Acid-etched samples showed greater oxygen contamination than those prepared by mechanical polishing. Heating the polished diamond to 1100 °C produced a surface that gave a (2×1) LEED pattern, but a (2×1) pattern was not observed after heating the acid-etched diamond. Hamza *et al.* observed that diamonds that do not reconstruct or reconstruct incompletely are those that show increased oxygen contamination.[14] Other than hydrogen, the principle contaminant of the diamond surface was graphitic carbon, which begins to appear after prolonged heating above 1025 °C.

No evidence of charging was apparent with the positron investigations due to the very low beam current of 0.6 pA. Sharp LEED patterns could be obtained with primary electron energies as low as 25 eV and beam currents of a few

mA. However, the peak positions on the Auger scans were shifted, indicating some sample charging does occur with a sufficiently intense and energetic electron beam and a room temperature sample.

The second diamond sample ($D2$), used for the Kelvin probe experiments, was a (100) oriented, type Ib, $4\times4\times0.25$ mm^3 diamond covered with a 0.5 μm-thick epilayer of boron-doped diamond. The diamond substrate was prepared for epilayer growth by first etching the substrate in hot acid using the procedure described above. The substrate was dipped in HF and rinsed with solvents prior to being loaded into the diamond growth reactor. The epilayer was grown by hot filament assisted CVD using methane, hydrogen, and diborane gases (C/H$=0.01$ and B/C$=5\times10^{-4}$) and $T_{\rm fil}=2000$ °C. The boron concentration in the diamond epilayer was $\sim2\times10^{19}$ cm^{-3}. Following growth, the sample was attached to a Mo mounting plate with silver epoxy and cured for 24 h at 150 °C in air. After loading the diamond into the test chamber, the system was evacuated and baked for 36 h; the chamber base pressure was less than 2×10^{-10} Torr. Auger electron spectroscopy (AES) showed a 1.5% atomic concentration of oxygen on the surface relative to carbon ($\sim$5% of a monolayer assuming a mean Auger probe depth of three monolayers) prior to the Kelvin probe measurements and a 1.2% atomic concentration of oxygen following the measurements.

III. RESULTS

Reemitted positron energy analysis

Positrons have a negative affinity for many materials;[26] the positron emission spectra from diamond, an example of which is shown in Fig. 3, indicate that the positron affinity for the (100) surface of diamond is negative as well. The positron affinity was taken to be the negative of the positron emission energy (corresponding to the peak of the differential distribution of total energy), less the contribution kT due to the positron thermal motion in the solid.[31] The analyzer potential (V_{A0}) that yields zero contact potential difference between the sample and analyzer defines the ''energy zero'' for our reemitted positron energy analyzer. At this potential the electric field between the analyzer and sample changes sign and positrons with very small velocity components in the normal direction are barely passed by the analyzer. In practice, this point is determined by measuring the transmitted positron flux for small analyzer voltages (V_A). If we assume the positron velocity in the normal direction ranges to zero, the inflection point between complete positron transmission and some repulsion defines the zero (Fig. 4). Because the contact potential difference changes with temperature and surface treatment, zero is defined for each energy measurement.

It is appropriate to consider explanations other than negative affinity to explain the positron emission. Epithermal emission or surface electric fields might cause positron emission from diamond, but cannot fully explain the observations. Epithermal positrons are positrons that are emitted before complete thermalization occurs. As shown in Fig. 3, the positrons are emitted nearly monoenergetically and there is little change between the normal and total energy differential spectrum, indicating that the positrons are emitted with little

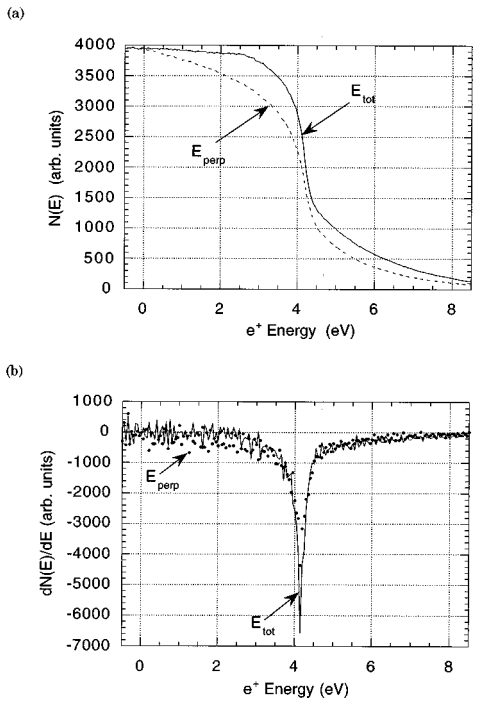

FIG. 3. (a) Integral and (b) differential spectra of positrons reemitted from the C(100) 1×1 surface vs. energy normal ($E_{\rm perp}$) to the surface. A second scan taken using the procedure discussed in the text yielded the *total* positron energy ($E_{\rm Tot}$) differential spectrum. The sample temperature was 425 °C for the two 6 V energy range scans. The zero energy point was obtained from the data shown in Fig. 4.

angular divergence.[32] The lack of angular divergence in the emission spectrum makes it unlikely that the emitted positrons are epithermal; epithermal positrons would have a nearly isotropic angular distribution. The populating of band-gap electron surface states and an accompanying distribution of near-surface ionized impurity atoms would produce a near-surface electric field. It is conceivable that the bottom of the positron band lies below the vacuum level at the surface (the work function would be positive) and a surface electric field raises the bulk positron band bottom above the vacuum level. However, the surface electric field would have to be active over a distance comparable to the positron mean-free-path in diamond to account for the narrow energy distribu-

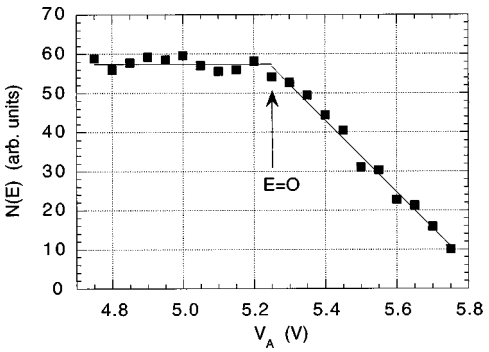

FIG. 4. High statistics positron energy scan used to determine the zero of the energy scale; the retarding electric field between the diamond sample and the particle detector changes sign at the point indicated by the arrow. The sample temperature was 425 °C for the high statistics, 0.4 V energy range scan.

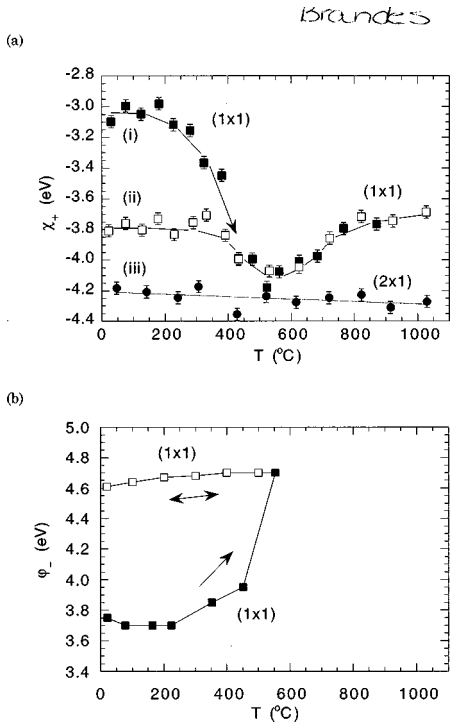

FIG. 5. (a) Positron affinity (or work function if $V_s=0$) vs. sample temperature for the 1×1 (squares) and 2×1 (circles) surfaces. The filled squares are data taken over a period of ~10 min after a ~1 s period of heating to at least 120 °C. The open squares are data taken immediately following a 20 s heating at 825 °C. The open square data point at 1025 °C was acquired from an acid etched surface that did not reconstruct. The slope of the line [curve (iii)] is (-0.20 ± 0.06) eV/1000 °C. If curve (i) represents a thermally activated surface change to the monohydride curve (ii) with an invariant LEED pattern, the activation energy is 1.2 eV. (b) Electron work function as a function of sample temperature. The electron work function at each temperature was obtained by assuming the Kelvin probe reference electrode has a work function of 4.2 eV and using data from Fig. 9.

tion in the positron differential emission energy scan and to eliminate the possibility that the positrons might decay into states below the vacuum level before emission. As we will discuss, an electric field that arises from populated gap surface states does exist at the (100) surface, but extends over many micrometers at room temperature. The principal *n*-type impurity in isopure diamonds is substitutional nitrogen, which has an activation energy of 1.7 eV. The number of ionized impurity atoms, even at a few hundred degrees C, is small enough that the depth of the surface electric field is micrometers, much greater than the positron mean free path, which is a few tens of angstroms.[33] Thus, we conclude that a positron negative affinity is the most likely explanation for our observations.

Our measurements of the positron work function as a function of sample temperature for different surface conditions are shown in Fig. 5(a). The positron data shown were taken at the temperatures indicated. The sequence of *ex situ* sample preparation, *in situ* heating, and work function measurement(s), described in greater detail below, was repeated many times and yielded statistically indistinguishable results.

The measurement results represented by filled squares in Fig. 5(a) were obtained from sample $D1$ following low-

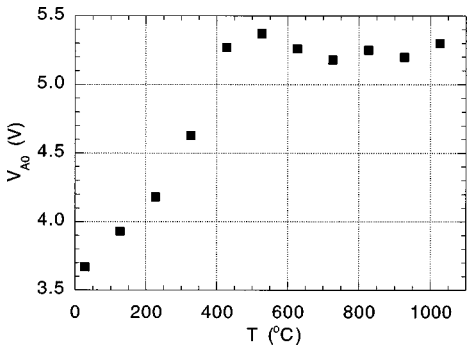

FIG. 6. Plot of the analyzer potential required to produce a zero field condition between the sample $D1$ surface and the particle detector as a function of sample temperature.

temperature heating to remove physisorbed contaminants prior to the measurement. This initial heating was typically to a temperature between 125 and 225 °C and always to a temperature less than 375 °C. After the initial heating, sample $D1$ exhibited a (1×1) LEED pattern. Subsequent to the initial heat treatment, the sample temperature was set and the positron work function measurement was performed. The (1×1) surface work function was -3.03 eV at 20 °C and dropped sharply when the sample temperature was above 325 °C. At intermediate temperatures, the (1×1) surface work function went through a minimum of -4.08 eV at (560 ± 50) °C and returned to -3.73 eV at higher temperatures. Curve (i), which represents the filled square data taken at temperatures below 400 °C, was not reversible and applies only for increasing temperature.

The measurement results represented by open squares in Fig. 5(a) were obtained from sample $D1$ following heating briefly to at least 725 °C, but no more than 975 °C, prior to measurement at temperature. Following this heat treatment, sample $D1$ exhibited a (1×1) LEED pattern. The open square data, which lies along curve (ii), were reversible. The positron work function was -3.73 eV at 20 °C. Curve (ii) has the same dip and asymptotic value as the filled square data taken at sample temperatures above 400 °C.

Upon heating the polished surface to >1250 °C a two-domain (2×1) LEED pattern was observed. The (2×1) surface work function was nearly constant, decreasing from -4.20 eV at 50 °C to -4.40 eV at 1025 °C [Figure 5(a)]. Curve (iii), a line fit to the data with a χ^2 per degree of freedom of $\chi^2/\nu=13/11$, had a slope of (-0.20 ± 0.06) eV/1000 °C. The data were reversible for curve (iii).

As discussed above, the analyzer voltage V_{A0} that produces no contact potential difference between the sample and the particle counter is identified (to set the energy scale zero) at each temperature. Figure 6 shows a plot of V_{A0} as a function of temperature from measurements that yielded some of the data shown in curve (ii), Fig. 5(a). A 1.6 V increase in the analyzer voltage was required to maintain zero contact potential difference when the sample was heated from room temperature to over 400 °C. A similar increase was required to maintain a zero contact potential difference with the 2×1 surface.

Reemitted positron yield studies

The diamond surface state population and surface electric field formation (band bending) was studied by implanting

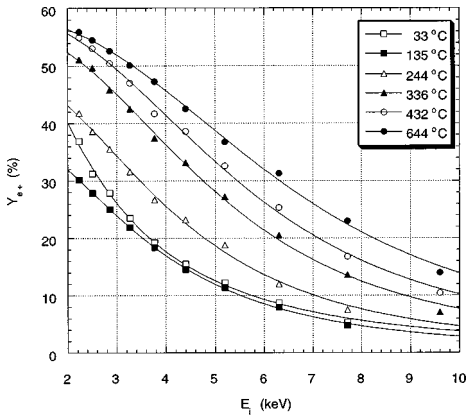

FIG. 7. Plot of slow positron yield as a function of positron implantation energy for different diamond $D1$ temperatures. Solid lines are a fit to the data using $Y_{e+}(E_i)=Y_0/[1-(E_i/E_0)]^n$ where Y_0, E_0, and n are fitting parameters.

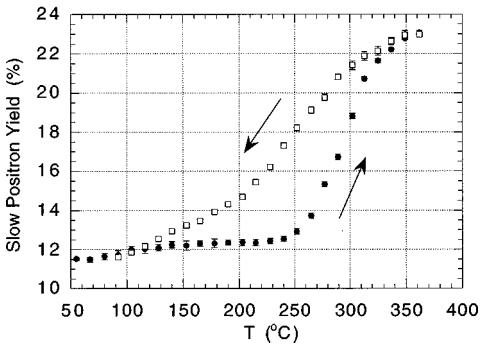

FIG. 8. The filled symbols indicate the slow positron yield when the sample is heated gradually. The open symbols indicate the slow positron yield upon cooling (heater turned off at T_{max}). The time to cool the sample was 1.6 times the time to heat the sample. The charge remains trapped in the surface states and is released primarily through a process associated with positron implantation and reemission.

monoenergetic, few keV positrons into the diamond sample and observing the reemitted positron fraction. The distribution of positrons in the sample following energy loss (thermalization) is a well characterized function of sample density and incident positron energy. Following thermalization the positrons diffuse through the crystal and if they encounter a negative positron affinity surface before they annihilate, they may be emitted into the vacuum. The presence of an internal electric field will alter the reemitted positron fraction by drifting more (or fewer) positrons to the surface.

The positron yield as a function of implantation energy increased with increasing sample temperature for the (1×1) surface (Fig. 7) and the (2×1) surface (not shown). We attribute the increase in positron yield to the formation of an electric field in the surface region. As the temperature is increased unoccupied surface states are populated with ionized donor electrons, producing a field that attracts positrons to the surface. By fitting the yield data to the diffusion equation with a field-dependent term,[34] we determined that an electric field on the order of 25 kV cm^{-1} was produced. Upon cooling, the surface-state population relaxes with a longer lifetime[35] due to the large energy scale of the wide band-gap semiconductor (Fig. 8).

Kelvin probe measurements

A Kelvin probe was used to measure the change in the contact potential and hence the electron work function, with temperature. A measurement consisted of heating the sample to a fixed temperature then measuring the contact potential difference as the sample cooled. Successively higher temperatures were examined. The contact potential difference between a polycrystalline Mo plate and the reference electrode was examined after each heating cycle to verify the reference electrode work function had not changed. A change in the reference electrode was observed when heating the sample to temperatures greater than 650 °C. Figure 9 shows measurements (diamond sample $D2$) of the CPD voltage ($V_{\text{offset}}^{\text{CPD}}$) that is applied directly to the grid ($eV_{\text{offset}}^{\text{CPD}}+\varphi_-^{\text{Au}}=\varphi_-^{\text{sample}}$). The Kelvin probe electronics took a few minutes to stabilize when turned on (immediately after the sample heater was turned off). The dashed lines in Fig. 9 show $V_{\text{offset}}^{\text{CPD}}$ extrapolated to the sample anneal temperature; the data below the lines were taken while the Kelvin probe stabilized. Because the shape of the data taken while the electronics stabilized was similar for all anneals below 650 °C and because the contact potential, once the electronics stabilized, changed little during cooling, we believe the curve extrapolated to the sample anneal temperature is an accurate representation of $V_{\text{offset}}^{\text{CPD}}$ during this period. The contact potential difference for a sample that sat in vacuum for several days was 0.22 V. Following heating to 163 °C the room-temperature contact potential difference was −0.42 V. Subsequent heating to successively higher temperatures increased the contact potential difference; the contact potential difference increased by ~0.8 V for a sample heated to 425 °C. At each temperature little change was observed in the contact potential difference upon cooling. The entire measurement sequence described above was repeated with statistically indistinguishable results.

Auger electron spectroscopy showed no appreciable change in the contamination of the surface. Display LEED showed a (1×1) spot pattern prior to heating; the LEED pattern and brightness did not change appreciably throughout the experiment. The observation of a clear LEED pattern without any heating of the sample and the AES results indi-

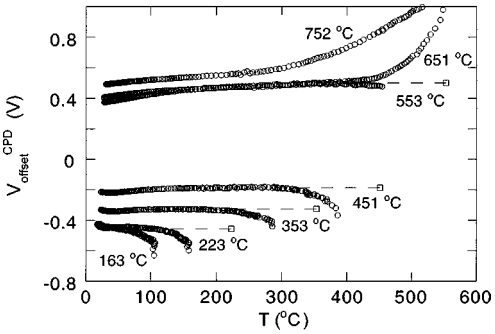

FIG. 9. Plot of the change in the Kelvin probe reference electrode potential required to maintain a zero field condition. Data was taken only while cooling sample (see discussion in text); numbers next to each curve indicate the annealing temperature before the start of each cooling/data acquisition cycle. The contact potential difference of the diamond surface contaminated with a thin layer of physisorbed contaminants was 0.22 V.

cate that any contaminant layer present at the start of the measurement is thin and composed of hydrogen or hydrocarbons. No incipient half order spots were observed upon heating to 750 °C.

Using the reference electrode workfunction $\varphi_{-}^{re}=4.2\pm0.2$ eV, the work function as a function of sample temperature, shown in Fig. 5(b), was calculated from the data shown in Fig. 9. The measurement results represented by filled squares in Fig. 5(b) were obtained as the sample was being heated; the filled square data were not reversible. The open square data were taken after the sample had been heated to 553 °C and the data along this curve were reversible. When heating to greater than ~575 °C the work function of the reference electrode may have changed and consequently, data from Kelvin probe measurements conducted above this temperature were not included in summary Fig. 5(b).

The room-temperature work function is 3.85 ± 0.2 eV after flashing and 4.75 ± 0.2 eV after heating to 725 °C with $\varphi_{-}^{re}=4.2\pm0.2$ eV. If the Fermi level coincides with diamond's boron level (0.35 eV above the valence band) then the electron affinity was -1.3 ± 0.2 eV after flashing (136 °C) and -0.4 ± 0.2 eV after heating to 725 °C.

Based upon the positron reemission measurements of the surface dipole, after heating hot enough to obtain a (2×1) LEED pattern, the surface dipole changes by roughly 0.45 V. This change in the dipole is enough to make the electron affinity of the (2×1) H-free surface positive, making it unlikely that thermalized electrons will escape at room temperature from the hydrogen-free surface, a result consistent with observations.[10,13]

Changes in the surface electric field [band bending, Fig. 2(b)], the surface dipole [Fig. 2(c)], or the chemical potential [Fig. 2(d)] will produce a change in the contact potential difference that can be readily detected. The chemical potential in sample $D2$, given the high dopant concentration, will not change substantially over the temperature range of these experiments. Therefore, changes in the contact potential as measured by the Kelvin probe are due to band bending and/or changes in the surface dipole. A comparison of the Kelvin probe measurement (contributions from band-bending and dipole) and the positron remission data (dipole only) shows that $\varphi_{-}(T)$ [Fig. 5(b)] is similar in magnitude, but opposite in sign, to $\chi_{+}(T)$ [Fig. 5(a)]. Consequently, although sample $D2$ is doped differently and has a differently prepared surface from that of sample $D1$, the change in the surface chemistry, and hence the surface dipole, is nearly the same. Although substantial band bending was observed with sample $D1$, little is observed with sample $D2$ (~0.15 eV), suggesting that how the surface is prepared determines the presence and location of surface states.

IV. DISCUSSION

Band bending

We now turn to the interpretation of our measurements. The increase in the fraction of positrons reemitted into the vacuum when sample $D1$ is heated provides clear evidence that an electric field forms in the surface region when the diamond is heated. The magnitude and penetration of the field are a function of the surface state charge density and the ionized impurity concentration in the bulk. We observe that implanted positrons are drifted towards the surface; the bands bend up as the surface is approached. Given the low positron yield at room temperature and the significant increase upon heating, $V_s<0.25$ V at room temperature.

With Kelvin probe measurements we cannot determine how much band bending exists at room temperature in sample $D2$. Following heating to greater than 400 °C we observe a 0.15 V change in the room temperature contact potential difference beyond that attributable to the surface dipole that we attribute to a change in band bending. Other researchers observed the room-temperature band bending for the as-grown, hydrogen plasma treated or atomic hydrogen/hot filament treated samples was less than 0.35 V for all but one tested sample.[23] Band bending upon removal of hydrogen[36–38] or upon oxygenation[13,39,40] tends to be as large as 2 V, the direction and magnitude being dependent in part upon the dopant type and concentration. Shirafuji and Sugino speculated[23] that bands in deep accumulation at the surface are responsible for diamond's anomalous low resistivity, but we find no evidence for a room temperature, deep accumulation mode in either diamond sample prepared by polishing, acid etching, or hot filament assisted CVD diamond growth.

We observe a reemitted positron yield of ~30% when positrons are implanted at 7.5 keV into sample $D1$ ($T_{\mathrm{samp}}=727$ °C). From fits of the yield data we estimate that the field in the surface region may be as large 25 kV cm^{-1}. Assuming a uniform field of 25 kV cm^{-1} over a mean implantation depth of $\bar{z}=(400/\rho)E^{1.6}=0.28\ \mu$m, where ρ is the density in gm cm^{-3} and $E=7.5$ kV is the implantation energy in kiloelectronvolts, we estimate the amount of band bending to be 0.7 V.[41] Upon heating from room temperature to 425 °C, the surface dipole changes by 0.25 V, the zero field point changes by 1.6 V (Fig. 6), and we calculate 0.7 V band bending. Therefore the Fermi level must shift towards the conduction band by 2.75 eV, a not unreasonable amount given diamond's wide band gap and sample $D1$'s low impurity concentration. Results from UPS studies showed the Fermi level of undoped CVD grown diamond was 0.9 eV above the valence band[42] and the single substitutional nitrogen level is 1.7 eV below the conduction band. If, as the sample is heated, the Fermi level shifts from low-density defect states 0.9 eV above the valence band to the nitrogen states, we would expect a shift of 2.9 eV, in good agreement with our measured and calculated shift of 2.75 eV. To produce a field of 25 kV cm^{-1}, the surface state charge density is approximately 3×10^{-9} C cm^{-2} corresponding to $3\times10^{10}e^{-}$ cm^{-2}, or about one surface state for every $\sim10^{5}$ surface carbon atoms.

The origin of the surface states is unclear. Hamza, Kubiak, and Stulen found no evidence of filled or empty surface states in hydrogenated diamond at room temperature, suggesting that intrinsic surface states are an unlikely explanation.[14] They did observe filled states up to 1.5 eV above the valence-band maximum on the π-bonded (2×1) surface. It is possible that the surface states are metastable, i.e., they form only at high temperature due to a change in the surface structure, but the surface states persisted after cooling, although the electron population in the states does not. The most likely explanation for the origin of the surface states is defect sites or the impurity oxygen. We see less

TABLE I. Changes in electron affinity (theoretical and experimental results) with changes in hydrogen coverage. The difference between the experimentally determined, fully hydrogenated surface affinity and the monohydride affinity is shown in the $\chi_{2H}-\chi_{1H}$ row, although the fully hydrogenated surface probably does not correspond to dihydride coverage.

	Verwoerd (Ref. 17)	van der Weide *et al.* (Ref. 18)	Furthmuller, Hafner and Kresse (Ref. 45)	e^+ reemission (this work)	Kelvin probe (this work)
$\chi_{1H}-\chi_{0H}$	−0.52	−3.0 eV	−0.94 eV	−0.44 eV	
$\chi_{2H}-\chi_{1H}$	−0.07	−1.2 eV		−0.73 eV	−0.86 eV

band bending with sample $D2$, but this sample also had a lower oxygen coverage and the epitaxial surface should be free of the defects found on the diamond polished surface. Photoemission studies showed downwards band bending upon oxidizing the type IIb, C(100) surface.[13,43,44] Heating to 1050 °C removed oxygen from the diamond surface.[18] The (2×1) surface, obtained by heating $D1$ to 1100 °C for 2 min., still had an attractive field at the surface for positrons. Therefore, oxygen was probably not the sole source of sample $D1$'s surface states; defect states may also play a role.

Surface chemistry, surface structure, and the effect on the surface dipole

We start by showing that the changes in the positron and electron work functions with temperature arise primarily from changes in the surface dipole. As discussed above, there was some band bending with samples $D1$ (~0.7 V) and $D2$ (~0.2 V) when the samples were heated and in the case of sample $D1$, a substantial shift in the Fermi level was observed. Unless the band bending is substantial over a distance comparable to the positron mean free path, the reemitted positron energy does not change substantially if surface electric fields are present. A shift in the electron Fermi level does not alter the positron affinity as the zero field point is determined every time. The positron affinity changes only with a change in the surface dipole or a change in the positron chemical potential.

From our measurements of the positron mobility we are able to assert that the positron chemical potential is relatively temperature independent and thus most of the changes exhibited in Fig. 5(a), curves (i) and (ii), are due to changes in the dipole potential $\Delta\phi$. The temperature-derivative of the positron chemical potential is the positron deformation potential $\varepsilon_d=\partial\mu_+/\partial V$ times the bulk modulus of diamond,[45]

$$\frac{\partial\mu_+}{\partial T}=\varepsilon_d\frac{\partial V}{\partial T}.$$

From the positron mobility in diamond[33] at 22 °C of (100 ± 10) cm^2 V^{-1} s^{-1} we find that $\varepsilon_d\approx25$ eV. Given the linear expansion coefficient of $\sim3\times10^{-6}$ K^{-1} we thus expect a change in μ_+ of only 0.25 eV for a 725 °C change in T. The slope of curve (iii) in Fig. 5(a) is in good agreement with this estimate. We conclude that the dipole potential of the (2×1) reconstructed surface, unlike the hydrogen terminated surface, is independent of temperature.

The Kelvin probe is sensitive to changes in the amount of band bending, shifts in the Fermi level, and changes in the surface dipole. Sample $D2$ was doped with boron, effectively locking the Fermi level into place ~0.35 eV above the valence band. As discussed above, the similar change with temperature of the negative of the electron work function and the positron affinity (Fig. 5) suggests that little band bending occurs in sample $D2$ and the changes observed with temperature are a consequence of changes in the surface dipole.

The relative temperature invariance of $\Delta\phi$ for a structure that is locked in place by reconstruction of the surface is not unexpected; only changes in the surface chemistry brought about by a change in hydrogen coverage are likely to noticeably alter the dipole potential. A similar change in the surface dipole is obtained with three different surface preps: as-grown surface, polishing with a diamond grit and olive oil slurry, or hot acid cleaning. Our results support the assessment that the (2×1) surface prepared by heating to greater than 1000 °C is hydrogen-free and consists of π-bonded dimers and contradict the assertion that the (2×1) surface produced by heating is composed of hydrogen terminated dimers. The increase in the surface dipole obtained from the positron measurements indicates that the (2×1) will be more positive by an additional 0.4–0.5 V, enough to change the electron affinity from negative to positive, as observed by other researchers,[10,13] and consistent with the removal of electropositive hydrogen.

The room temperature values of $\Delta\phi$, assuming the H electrons are closer to the surface than the protons, that is, they are participating in paired electron bonding, should increase in response to an increase in the hydrogen coverage (Table I).[17,18,46] The positron affinity should therefore increase (become less negative) by an equal amount upon hydrogenation. Our measurements agree with the trend—the positron affinity increases with increasing hydrogen coverage—if we assume that H desorbs as the sample is subjected to higher temperatures. Based upon the experimental and theoretical studies discussed in the introduction, the fully hydrogenated surface used to obtain the low temperature results shown in Fig. 5(a) curve (i), corresponds to coverage substantially greater than one hydrogen atom per surface carbon [Figs. 1(a), 1(b), or 1(c)]. The temperature at which hydrogen starts to desorb from the hydrogen-saturated surface is ~350 °C. Enough hydrogen and disorder remains upon heating the sample to 725 °C to prevent conversion to the ordered 2×1 dimer-bonded surface. The remaining hydrogen is of order one H per surface carbon [Fig. 1(d) or 1(e)]. We believe curve (ii) corresponds to the disordered, 2×1, monohydride terminated surface.[4,7] The increase at 22 °C of 0.44 eV in the positron affinity between curves (iii) and (ii), and the increase of 1.17 eV between curves (iii) and (i) is in qualitative agreement with the theoretical results. The affinity measurements are most readily explained by an as-prepared surface that contains substantially more than one

hydrogen atom per surface carbon, an annealed 350 °C surface that contains approximately one hydrogen atom per surface carbon, and an annealed above 1000 °C, 2×1 π-bonded surface that is essentially hydrogen-free.

Observing a (1×1) LEED pattern does not guarantee that the surface has (1×1) symmetry.[47] A surface with hydrogen coverage between 1.5 and 2.0 H per surface carbon would not reconstruct appreciably and would exhibit a (1×1) LEED pattern. Researchers have suggested that a disordered phase (consisting of randomly oriented $[(2n+1)\times1]$ cells composed of hydrogen terminated dimers and a dihydride terminated carbon) could exist on the diamond (100) surface and the (1×1) pattern could arise from underlying layers.[3] No fractional order spots were visible and the diffraction spots in our display LEED appeared bright and well defined, but a careful analysis of the spot profile would be required to conclusively determine the existence of a disordered overlayer. We cannot rule out that hydrocarbon contaminants are covering the surface when we took the data plotted in Fig. 5(a), curve (i), but the LEED spot intensity and shape, the relative chemical inertness of the diamond, and the ease with which one should be able to remove physisorbed contaminants (<250 °C), and striking similarity between the positron and electron data (Fig. 5) suggests that chemically bonded hydrogen is responsible for the result.

The most surprising observation is the dip in χ_+ that occurs at 575 °C for the disordered (2×1) monohydride surface. It may be that the hydrogen atoms become delocalized on the diamond surface at a certain temperature,[48–52] thus leading to a small change in $\Delta\phi$, but it would be hard to use this mechanism to fully explain curve (ii), Fig. 5(a). On the other hand, the overlayer may be exhibiting order-disorder transitions. Consider, as an example, the simplistic case where there is no dimer bonding and hydrogen coverage corresponds to one H per surface carbon atom. The surface could be an example of an anisotropic 2D Ising system[53] with the ground state being either the ''ferromagnetic'' or ''antiferromagnetic'' state illustrated in Figs. 10(a) and 10(b). When such a system is heated it will melt first in one dimension [Fig. 10(c)] and then in both dimensions [Fig. 10(d)]. At a high enough temperature there could be a transition to the gaseous state that has no analog in the simple Ising model. It is interesting to speculate that fluctuations or phase transitions could be responsible for the observed dip in χ_+, but in any case, it is clear that our measurements would provide a useful test for different atomistic calculations of the diamond surface configurations. Unfortunately, because the sample heating changed the reference electrode potential when heating to greater than 553 °C, we could not explore the change in φ_- over the 450 to 750 °C temperature range where the dip in χ_+ is observed.

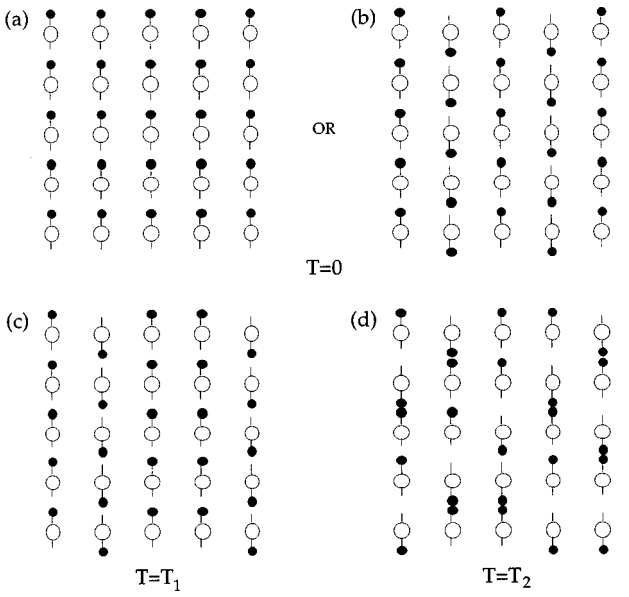

FIG. 10. Possible configurations of the H atoms in the monohydride terminated diamond (100) surface. Configurations (a)–(d) correspond to states of an anisotropic 2D Ising system at successively higher temperatures. The ground state is either ''ferromagnetic'' (a) or ''antiferromagnetic'' (b). In (c) and (d) the system melts first in one dimension at T_1 and then in two dimensions at T_2. The large temperature gaseous nonIsing configuration might not be realizable without complete hydrogen desorption occurring.

V. CONCLUSIONS

In conclusion, we observe the following.

The positron affinity χ_+ of diamond (100) surfaces is negative. When diamond is heated to less than 300 °C, $\chi_+ = -3.03\pm0.04$ eV (room temperature, 1×1 LEED pattern); when heated to over 450 but less than 1000 °C, $\chi_+ = -3.76\pm0.04$ eV (room temperature, 1×1 LEED pattern); and when heated to greater than 1000 °C, $\chi_+ = -4.20\pm0.04$ eV (room temperature, 2×1 LEED pattern).

The electron affinity of diamond surface heated to less than 750 °C is negative. For diamond heated to less than 300 °C, $\varphi_- = -3.03\pm0.04$ eV (room temperature, 1×1 LEED pattern), and when heated to over 450 but less than 1000 °C, $\varphi_- = -3.76\pm0.04$ eV (room temperature, 1×1 LEED pattern).

The work-function measurements are most readily explained by an as-prepared surface that contains substantially more than one hydrogen atom per surface carbon, an annealed 350 °C surface that contains approximately one hydrogen atom per surface carbon, and an annealed above 1000 °C, 2×1 π-bonded surface that is essentially hydrogen-free. The decreases in the room-temperature values of χ_+ and increases in room temperature values of φ_- as hydrogen is removed are in agreement with previous theoretical results.

The (2×1) surface work function is nearly temperature independent, indicative of a surface that is nearly hydrogen-free and most likely consists of π-bonded dimers. As the temperature is raised, the work function of the (1×1) partially hydrogenated surface decreases to a minimum of -4.08 eV at (560 ± 50) °C and returns to the room temperature value by 825 °C. We speculate that the complex temperature dependence is caused by fluctuations or phase transitions of the 2D array of hydrogen atoms.

Two differently doped diamonds prepared with three different techniques: grit and olive oil polishing, hot acid cleaning, and hot filament assisted chemical vapor deposition growth showed little band bending at room temperature. A

positive, outward-directed electric field formed at high temperatures at the surface of a diamond prepared with polishing or acid cleaning. Polishing defects and/or oxygen on the surface are likely to produce the surface states that create the electric field. The surface state charge density was greater than $3\times10^{10}\ e^-\ \mathrm{cm}^{-2}$.

ACKNOWLEDGMENTS

The authors would like to thank K. F. Canter, D. R. Hamann, P. B. Littlewood, X. Xu, and J. B. Miller for interesting discussions. This work was supported in part by NSF Grant No. DMI-9505418 and BMDO Grant No. N00014-96-C-0266.

*Electronic address: grb@atmi.com

[1] *Handbook of Industrial Diamonds and Diamond Films*, edited by M. A. Prelas, G. Popovici, and L. K. Bigelow (Dekker, New York, 1997).

[2] G. R. Brandes, in *Handbook of Industrial Diamonds and Diamond Films* (Ref. 1).

[3] Y. L. Yang and M. P. D'Evelyn, J. Am. Chem. Soc. **114**, 2797 (1992).

[4] T. Aizawa, T. Ando, M. Kamo, and Y. Sato, Phys. Rev. B **48**, 18 348 (1993).

[5] B. D. Thoms, M. S. Owen, J. E. Butler, and C. Spiro, Appl. Phys. Lett. **65**, 2957 (1994).

[6] P. G. Lurie and J. M. Wilson, Surf. Sci. **4**, 241 (1966).

[7] M. Sternberg, Th. Fraunheim, W. Zimmerman-Edling, and H. G. Busmann, Surf. Sci. **370**, 232 (1997).

[8] R. E. Thomas, R. A. Rudder, and R. J. Markunas, J. Vac. Sci. Technol. A **10**, 2451 (1992).

[9] B. D. Thoms and J. E. Butler, Surf. Sci. **328**, 291 (1995).

[10] P. K. Baumann and R. J. Nemanich, Diamond Relat. Mater. **4**, 802 (1995).

[11] C. Nutzenadel, O. M. Kuettel, L. Diederich, E. Maillard-Schuller, O. Groening, and L. Schlapbach, Surf. Sci. Lett. **369**, L111 (1996).

[12] O. M. Kuttel, L. Diederich, E. Schaller, O. Carnal, and L. Schlapbach, Surf. Sci. Lett. **337**, L812 (1995).

[13] R. E. Thomas, T. P. Humphreys, C. Pettenkofer, D. P. Malta, J. B. Posthill, M. J. Mantini, R. A. Rudder, G. C. Hudson, and R. J. Markunas, in *Diamond for Electronic Applications*, edited by D. Dreifus *et al.*, MRS Symposia Proceedings No. 416 (Materials Research Society, Pittsburgh, 1996), p. 263.

[14] A. V. Hamza, G. D. Kubiak, and R. H. Stulen, Surf. Sci. **237**, 35 (1990), and references therein. See also G. D. Kubiak, M. T. Schulberg, and R. H. Stulen, *ibid.* **277**, 234 (1992).

[15] S. Y. Yang, D. A. Drabold, and J. B. Adams, Phys. Rev. B **48**, 5261 (1993).

[16] T. Frauenheim, P. Blaudeck, and D. Porezag, in *Novel Forms of Carbon Symposium*, edited by C. L. Renschler, J. J. Pouch, and D. M. Cox (Materials Research Society, Pittsburgh, 1992), p. 395.

[17] W. S. Verwoerd, Surf. Sci. **108**, 153 (1981).

[18] J. van der Weide, Z. Zhang, P. K. Baumann, G. M. Wensell, J. Bernholc, and R. J. Nemanich, Phys. Rev. B **50**, 5803 (1994).

[19] G. T. Mearini, I. L. Krainsky, and J. A. Dayton, Jr., Surf. Interface Anal. **21**, 138 (1994).

[20] M. I. Landstross and K. V. Ravi, Appl. Phys. Lett. **55**, 975 (1989).

[21] S. Albin and L. Watkins, Appl. Phys. Lett. **56**, 1454 (1990).

[22] S. A. Grot, G. S. Gildenblat, C. W. Hatfield, C. R. Wronski, A. R. Badzian, T. Badzian, and R. Messier, IEEE Electron Device Lett. **11**, 100 (1990).

[23] J. Shirafuji and T. Sugino, Diamond Relat. Mater. **5**, 706 (1996).

[24] A. P. Mills, Jr., in *Positron Spectroscopy of Solids*, edited by A. Dupasquier and A. P. Mills, Jr. (IOS, Amsterdam, 1995), 209.

[25] Due to experimental difficulties in separating contributions from the surface dipole and band bending, $\Delta\phi$ and qVs are sometimes grouped together and called the ''dipole term.''

[26] See, for example, P. J. Schultz and K. G. Lynn, Rev. Mod. Phys. **60**, 701 (1988), and references therein.

[27] W. B. Hermannsfeldt (unpublished).

[28] E. M. Gullikson, A. P. Mills, Jr., W. S. Crane, and B. L. Brown, Phys. Rev. B **32**, 5484 (1985).

[29] G. F. Saville, P. M. Platzman, G. R. Brandes, Rene Ruel, and R. L. Willet, J. Vac. Sci. Technol. B **13**, 2184 (1995).

[30] D. E. Eastman, Phys. Rev. B **2**, 1 (1970).

[31] E. M. Gullikson and A. P. Mills, Jr., Phys. Rev. Lett. **57**, 376 (1986).

[32] Preliminary results of our study of the (100) surface of diamond were presented in G. R. Brandes, A. P. Mills, Jr., and D. M. Zuckerman, Mater. Sci. Forum **105-110**, 1363 (1992).

[33] A. P. Mills, Jr., G. R. Brandes, D. M. Zuckerman, W. Liu, and S. Berko, Mater. Sci. Forum **105-110**, 763 (1992).

[34] A. P. Mills, Jr. and C. A. Murray, Appl. Phys. **21**, 323 (1980).

[35] A. Many, Y. Goldstein, and N. B. Grover, *Semiconductor Surfaces* (Elsevier, New York, 1971).

[36] L. Diederich, O. Kuttel, E. Schaller, and L. Schlapbach, Surf. Sci. **349**, 176 (1996).

[37] J. Wu, R. Cao, X. Yang, P. Pianetta, and I. Lindau, J. Vac. Sci. Technol. A **11**, 1048 (1993).

[38] V. S. Smentkowski, H. Jansch, M. A. Henderson, and J. T. Yates, Surf. Sci. **330**, 207 (1995).

[39] T. Sugino and J. Shirafuji, Phys. Status Solidi A **154**, 371 (1996).

[40] P. E. Pehrsson, J. P. Long, M. J. Marchywka, and J. E. Butler, Appl. Phys. Lett. **67**, 3414 (1996).

[41] S. Valkaelahti and R. M. Nieminen, Appl. Phys. A: Solids Surf. **35**, 51 (1984).

[42] R. Graupner, R. Stockel, K. Janischowski, J. Ristein, M. Hundhausen, and L. Ley, Diamond Relat. Mater. **3**, 891 (1994).

[43] T. Sugino and J. Shirafuji, Phys. Status Solidi A **154**, 371 (1996).

[44] P. E. Pehrsson, J. P. Long, M. J. Marchywka, and J. E. Butler, Appl. Phys. Lett. **67**, 3414 (1996).

[45] E. M. Gullikson and A. P. Mills, Jr., Phys. Rev. B **35**, 8759 (1987).

[46] J. Furthmuller, J. Hafner, and G. Kresse, Phys. Rev. B **53**, 7334 (1996).

[47] Y. J. Chabal and K. Raghavachari, Phys. Rev. Lett. **54**, 1055 (1985).

[48] S. C. Wang and R. Gomer, J. Chem. Phys. **83**, 4193 (1985), and references therein.

[49] C. M. Mate and G. A. Somorjai, Phys. Rev. B **34**, 7417 (1986).

[50] J. W. Chung, K. Evans-Lutterodt, E. D. Spect, R. J. Birgeneau, P. J. Estrup, and A. R. Kortan, Phys. Rev. Lett. **59**, 2192 (1987).

[51] K. Sinniah, M. G. Sherman, L. B. Lewis, W. H. Weinberg, J. T. Yates, Jr., and K. C. Janda, Phys. Rev. Lett. **62**, 567 (1989).

[52] C. Astaldi, A. Bianco, S. Modesti, and E. Tosatti, Phys. Rev. Lett. **68**, 90 (1992).

[53] G.-C. Wang and T.-M. Lu, Phys. Rev. B **31**, 5918 (1985).